

Densely sampled viral trajectories suggest longer duration of acute infection with B.1.1.7 variant relative to non-B.1.1.7 SARS-CoV-2

Stephen M. Kissler*¹, Joseph R. Fauver*², Christina Mack*^{3,4}, Caroline G. Tai³, Mallery I. Breban², Anne E. Watkins², Radhika M. Samant³, Deverick J. Anderson⁵, David D. Ho⁶, Nathan D. Grubaugh^{†2}, Yonatan H. Grad^{†1}

¹ Department of Immunology and Infectious Diseases, Harvard T.H. Chan School of Public Health, Boston, MA

² Department of Epidemiology of Microbial Diseases, Yale School of Public Health, New Haven, CT

³ IQVIA, Real World Solutions, Durham, NC

⁴ Department of Epidemiology, University of North Carolina-Chapel Hill, Chapel Hill, NC

⁵ Duke Center for Antimicrobial Stewardship and Infection Prevention, Durham, NC

⁶ Aaron Diamond AIDS Research Center, Columbia University Vagelos College of Physicians and Surgeons, New York, NY

* denotes equal contribution

† denotes co-senior authorship

Correspondence and requests for materials should be addressed to:

Email: ygrad@hsph.harvard.edu

Telephone: 617.432.2275

Abstract.

To test whether acute infection with B.1.1.7 is associated with higher or more sustained nasopharyngeal viral concentrations, we assessed longitudinal PCR tests performed in a cohort of 65 individuals infected with SARS-CoV-2 undergoing daily surveillance testing, including seven infected with B.1.1.7. For individuals infected with B.1.1.7, the mean duration of the proliferation phase was 5.3 days (90% credible interval [2.7, 7.8]), the mean duration of the clearance phase was 8.0 days [6.1, 9.9], and the mean overall duration of infection (proliferation plus clearance) was 13.3 days [10.1, 16.5]. These compare to a mean proliferation phase of 2.0 days [0.7, 3.3], a mean clearance phase of 6.2 days [5.1, 7.1], and a mean duration of infection of 8.2 days [6.5, 9.7] for non-B.1.1.7 virus. The peak viral concentration for B.1.1.7 was 19.0 Ct [15.8, 22.0] compared to 20.2 Ct [19.0, 21.4] for non-B.1.1.7. This converts to 8.5 log₁₀ RNA copies/ml [7.6, 9.4] for B.1.1.7 and 8.2 log₁₀ RNA copies/ml [7.8, 8.5] for non-B.1.1.7. These data offer evidence that SARS-CoV-2 variant B.1.1.7 may cause longer infections with similar peak viral concentration compared to non-B.1.1.7 SARS-CoV-2. This extended duration may contribute to B.1.1.7 SARS-CoV-2's increased transmissibility.

43 **Main text.**

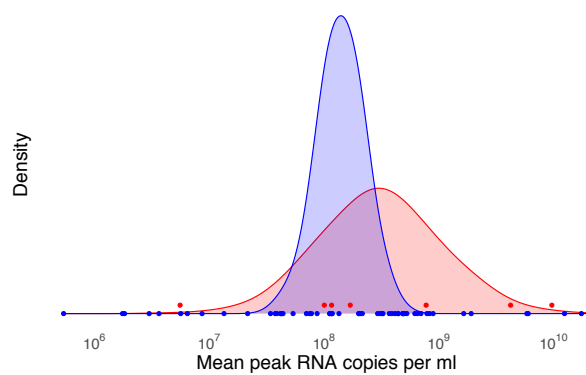
44 The reasons for the enhanced transmissibility of SARS-CoV-2 variant B.1.1.7 are unclear. B.1.1.7
45 features multiple mutations in the spike protein receptor binding domain¹ that may enhance ACE-
46 2 binding², thus increasing the efficiency of virus transmission. A higher or more persistent viral
47 burden in the nasopharynx could also increase transmissibility. To test whether acute infection
48 with B.1.1.7 is associated with higher or more sustained nasopharyngeal viral concentrations, we
49 assessed longitudinal PCR tests performed in a cohort of 65 individuals infected with SARS-CoV-
50 2 undergoing daily surveillance testing, including seven infected with B.1.1.7, as confirmed by
51 whole genome sequencing.

52
53 We estimated (1) the time from first detectable virus to peak viral concentration (proliferation time),
54 (2) the time from peak viral concentration to initial return to the limit of detection (clearance time),
55 and (3) the peak viral concentration for each individual (**Supplementary Appendix**).³ We esti-
56 mated the means of these quantities separately for individuals infected with B.1.1.7 and non-
57 B.1.1.7 SARS-CoV-2 (**Figure 1**). For individuals infected with B.1.1.7, the mean duration of the
58 proliferation phase was 5.3 days (90% credible interval [2.7, 7.8]), the mean duration of the clear-
59 ance phase was 8.0 days [6.1, 9.9], and the mean overall duration of infection (proliferation plus
60 clearance) was 13.3 days [10.1, 16.5]. These compare to a mean proliferation phase of 2.0 days
61 [0.7, 3.3], a mean clearance phase of 6.2 days [5.1, 7.1], and a mean duration of infection of 8.2
62 days [6.5, 9.7] for non-B.1.1.7 virus. The peak viral concentration for B.1.1.7 was 19.0 Ct [15.8,
63 22.0] compared to 20.2 Ct [19.0, 21.4] for non-B.1.1.7. This converts to 8.5 log₁₀ RNA copies/ml
64 [7.6, 9.4] for B.1.1.7 and 8.2 log₁₀ RNA copies/ml [7.8, 8.5] for non-B.1.1.7. Data and code are
65 available online.⁴

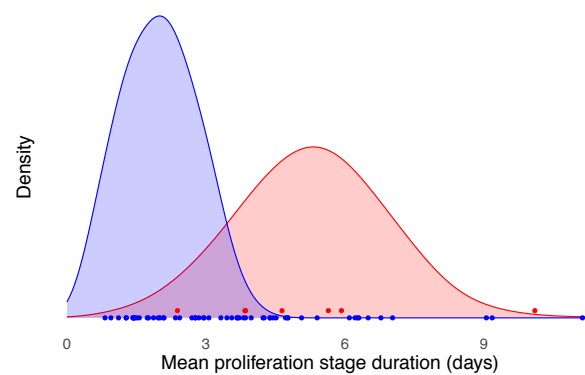
66
67 These data offer evidence that SARS-CoV-2 variant B.1.1.7 may cause longer infections with
68 similar peak viral concentration compared to non-B.1.1.7 SARS-CoV-2, and this extended dura-
69 tion may contribute to B.1.1.7 SARS-CoV-2's increased transmissibility. The findings are prelimi-
70 nary, as they are based on seven B.1.1.7 cases. However, if borne out by additional data, a longer
71 isolation period than the currently recommended 10 days after symptom onset⁵ may be needed
72 to effectively interrupt secondary infections by this variant. Collection of longitudinal PCR and test
73 positivity data in larger and more diverse cohorts is needed to clarify the viral trajectory of variant
74 B.1.1.7. Similar analyses should be performed for other SARS-CoV-2 variants such as B.1.351
75 and P.1.

76

A)



B)

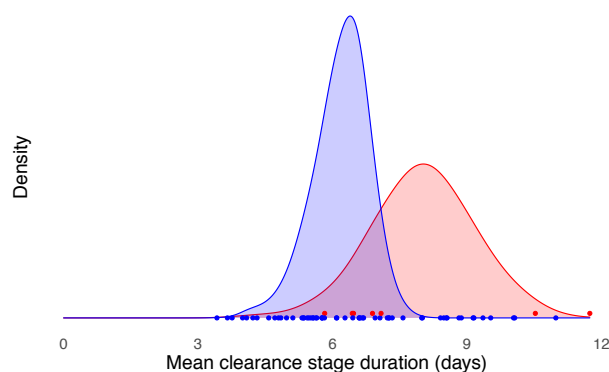


77

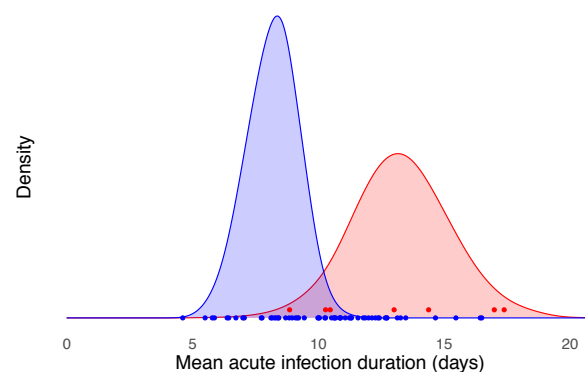
78

79

C)



D)



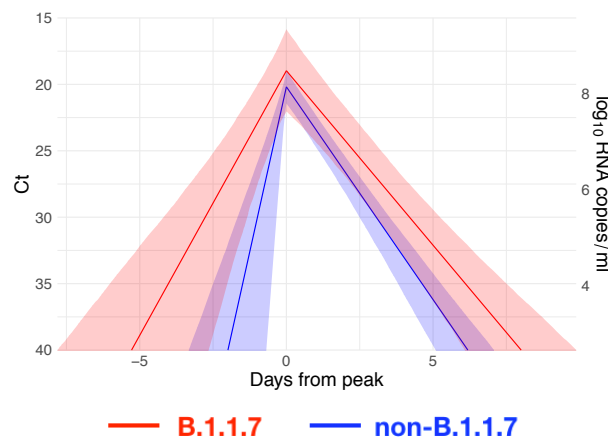
80

81

82

83

E)



84

85

86

87 **Figure 1. Estimated viral trajectories for B.1.1.7 and non-B.1.1.7 SARS-CoV-2.** Posterior distributions for the mean
88 peak viral concentration (A), mean proliferation duration (B), mean clearance duration (C), mean total duration of acute
89 infection (D), and mean posterior viral concentration trajectory (E) for the B.1.1.7 variant (red) and non-B.1.1.7 SARS-
90 CoV-2 (blue). In (A)–(D), distributions depict kernel density estimates obtained from 2,000 draws from the posterior
91 distributions for each statistic. Points depict the individual-level posterior means for each statistic. In (E), solid lines
92 depict the estimated mean viral trajectory. Shaded bands depict the 90% credible intervals for the mean viral trajectory.
93

References

1. Galloway SE, Paul P, MacCannell DR, Johansson MA, Brooks JT, MacNeil A, et al. Emergence of SARS-CoV-2 B.1.1.7 Lineage — United States, December 29, 2020–January 12, 2021. *MMWR Morb Mortal Wkly Rep.* 2021;70(3):95-99. doi:10.15585/mmwr.mm7003e2
2. Yi C, Sun X, Ye J, Ding L, Liu M, Yang Z, et al. Key residues of the receptor binding motif in the spike protein of SARS-CoV-2 that interact with ACE2 and neutralizing antibodies. *Cell Mol Immunol.* 2020;17(6):621-630. doi:10.1038/s41423-020-0458-z
3. Kissler SM, Fauver JR, Mack C, Olesen SW, Tai C, Shiue KY, et al. SARS-CoV-2 viral dynamics in acute infections. *medRxiv.* Published online 2020:1-13. doi:10.1101/2020.10.21.20217042
4. Kissler S. Github Repository: CtTrajectories_B117. Published 2020. Accessed February 8, 2020. https://github.com/skissler/CtTrajectories_B117
5. Centers for Disease Control and Prevention. Duration of Isolation and Precautions for Adults with COVID-19. COVID-19. Published 2020. Accessed February 8, 2020. <https://www.cdc.gov/coronavirus/2019-ncov/hcp/duration-isolation.html>
6. Fauver JR, Petrone ME, Hodcroft EB, Shioda K, Ehrlich HY, Watts AG, et al. Coast-to-Coast Spread of SARS-CoV-2 during the Early Epidemic in the United States. *Cell.* 2020;181(5):990-996.e5. doi:10.1016/j.cell.2020.04.021
7. Loman N, Rowe W, Rambaut A. nCoV-2019 novel coronavirus bioinformatics protocol.
8. Rambaut A, Holmes EC, O'Toole Á, Hill V, McCrone JT, Ruis C, et al. A dynamic nomenclature proposal for SARS-CoV-2 lineages to assist genomic epidemiology. *Nat Microbiol.* 2020;5(11):1403-1407. doi:10.1038/s41564-020-0770-5
9. Rambaut A, Loman N, Pybus O, Barclay W, Barrett J, Carabelli A, et al. *Preliminary Genomic Characterisation of an Emergent SARS-CoV-2 Lineage in the UK Defined by a Novel Set of Spike Mutations.*; 2020.
10. Kudo E, Israelow B, Vogels CBF, Lu P, Wyllie AL, Tokuyama M, et al. Detection of SARS-CoV-2 RNA by multiplex RT-qPCR. Sugden B, ed. *PLOS Biol.* 2020;18(10):e3000867. doi:10.1371/journal.pbio.3000867
11. Vogels C, Fauver J, Ott IM, Grubaugh N. *Generation of SARS-COV-2 RNA Transcript Standards for QRT-PCR Detection Assays.*; 2020. doi:10.17504/protocols.io.bdv6i69e
12. Cleary B, Hay JA, Blumenstiel B, Gabriel S, Regev A, Mina MJ. Efficient prevalence estimation and infected sample identification with group testing for SARS-CoV-2. *medRxiv.* Published online 2020.
13. Tom MR, Mina MJ. To Interpret the SARS-CoV-2 Test, Consider the Cycle Threshold Value. *Clin Infect Dis.* 2020;02115(Xx):1-3. doi:10.1093/cid/ciaa619
14. Carpenter B, Gelman A, Hoffman MD, Lee D, Goodrich B, Betancourt M, et al. Stan : A Probabilistic Programming Language. *J Stat Softw.* 2017;76(1). doi:10.18637/jss.v076.i01
15. R Development Core Team R. R: A Language and Environment for Statistical Computing. Team RDC, ed. *R Found Stat Comput.* 2011;1(2.11.1):409. doi:10.1007/978-3-540-74686-7

137 **Supplementary Appendix.**

138

139 Ethics.

140 Residual de-identified viral transport media from anterior nares and oropharyngeal swabs
141 collected from players, staff, vendors, and associated household members from a professional
142 sports league were obtained from BioReference Laboratories. In accordance with the guidelines
143 of the Yale Human Investigations Committee, this work with de-identified samples was approved
144 for research not involving human subjects by the Yale Internal Review Board (HIC protocol #
145 2000028599). This project was designated exempt by the Harvard IRB (IRB20-1407).

146

147 Study population. The data reported here represent a convenience sample including team staff,
148 players, arena staff, and other vendors (e.g., transportation, facilities maintenance, and food
149 preparation) affiliated with a professional sports league. Clinical samples were obtained by
150 combined swabs of the anterior nares and oropharynx administered by a trained provider. Viral
151 concentration was measured using the cycle threshold (Ct) according to the Roche cobas target
152 1 assay. For an initial pool of 298 participants who first tested positive for SARS-CoV-2 infection
153 during the study period (between November 28th, 2020 and January 20th, 2021), a diagnosis of
154 “novel” or “persistent” infection was recorded. “Novel” denoted a likely new infection while
155 “persistent” indicated the presence of virus in a clinically recovered individual. A total of 65
156 individuals (90% male) had novel infections that met our inclusion criteria: at least five positive
157 PCR tests (Ct < 40) and at least one test with Ct < 35. Seven of these individuals were infected
158 with the B.1.1.7 variant as confirmed by genomic sequencing.

159

160 Genome sequencing and lineage assignments: RNA was extracted from remnant
161 nasopharyngeal diagnostic specimens and used as input for SARS-CoV-2 genomic sequencing
162 as previously described.⁶ Samples were sequenced on the Oxford Nanopore MinION. Consensus
163 sequences were generated using the ARTIC Network analysis pipeline⁷ and samples with >80%
164 genome coverage were included in analysis. Individual SARS-CoV-2 genomes were assigned to
165 PANGO lineages using Pangolin v.2.1.8.⁸ All viral genomes assigned to the B.1.1.7 lineage were
166 manually examined for representative mutations.⁹

167

168 Converting Ct values to viral genome equivalents. To convert Ct values to viral genome
169 equivalents, we first converted the Roche cobas target 1 Ct values to equivalent Ct values on a

170 multiplexed version of the RT-qPCR assay from the US Centers for Disease Control and
171 Prevention.¹⁰ We did this following our previously described methods.³ Briefly, we adjusted the
172 Ct values using the best-fit linear regression between previously collected Roche cobas target 1
173 Ct values and CDC multiplex Ct values using the following regression equation:

174

$$175 \quad y_i = \beta_0 + \beta_1 x_i + \epsilon_i$$

176

177 Here, y_i denotes the i^{th} Ct value from the CDC multiplex assay, x_i denotes the i^{th} Ct value from the
178 Roche cobas target 1 test, and ϵ_i is an error term with mean 0 and constant variance across all
179 samples. The coefficient values are $\beta_0 = -6.25$ and $\beta_1 = 1.34$.

180

181 Ct values were fitted to a standard curve in order to convert Ct value data to RNA copies. Synthetic
182 T7 RNA transcripts corresponding to a 1,363 b.p. segment of the SARS-CoV-2 nucleocapsid gene
183 were serially diluted from 10^6 - 10^0 RNA copies/ μl in duplicate to generate a standard curve¹¹
184 **(Supplementary Table 1)**. The average Ct value for each dilution was used to calculate the slope
185 (-3.60971) and intercept (40.93733) of the linear regression of Ct on log-10 transformed standard
186 RNA concentration, and Ct values from subsequent RT-qPCR runs were converted to RNA copies
187 using the following equation:

188

$$189 \quad \log_{10}([\text{RNA}]) = (Ct - 40.93733)/(-3.60971) + \log_{10}(250)$$

190

191 Here, [RNA] represents the RNA copies /ml. The $\log_{10}(250)$ term accounts for the extraction (300
192 μl) and elution (75 μl) volumes associated with processing the clinical samples as well as the
193 1,000 $\mu\text{l}/\text{ml}$ unit conversion.

194

195 Model fitting.

196 For the statistical analysis, we removed any sequences of 3 or more consecutive negative tests
197 to avoid overfitting to these trivial values. Following our previously described methods,³ we
198 assumed that the viral concentration trajectories consisted of a proliferation phase, with
199 exponential growth in viral RNA concentration, followed by a clearance phase characterized by
200 exponential decay in viral RNA concentration.¹² Since Ct values are roughly proportional to the
201 negative logarithm of viral concentration¹³, this corresponds to a linear decrease in Ct followed by
202 a linear increase. We therefore constructed a piecewise-linear regression model to estimate the

203 peak Ct value, the time from infection onset to peak (*i.e.* the duration of the proliferation stage),
204 and the time from peak to infection resolution (*i.e.* the duration of the clearance stage). The
205 trajectory may be represented by the equation

$$E[Ct(t)] = \begin{cases} \text{l.o.d.} & t \leq t_o \\ \text{l.o.d.} - \frac{\delta}{t_p - t_o}(t - t_o) & t_o < t \leq t_p \\ \text{l.o.d.} - \delta + \frac{\delta}{t_r - t_p}(t - t_p) & t_p < t \leq t_r \\ \text{l.o.d.} & t > t_r \end{cases}$$

207
208
209 Here, $E[Ct(t)]$ represents the expected value of the Ct at time t , “l.o.d” represents the RT-qPCR
210 limit of detection, δ is the absolute difference in Ct between the limit of detection and the peak
211 (lowest) Ct, and t_o , t_p , and t_r are the onset, peak, and recovery times, respectively.

212
213 Before fitting, we re-parametrized the model using the following definitions:

- 214
- 215 • $\Delta Ct(t) = \text{l.o.d.} - Ct(t)$ is the difference between the limit of detection and the observed Ct
216 value at time t .
 - 217 • $\omega_p = t_p - t_o$ is the duration of the proliferation stage.
 - 218 • $\omega_c = t_r - t_p$ is the duration of the clearance stage.

219
220 We constrained $0.25 \leq \omega_p \leq 14$ days and $2 \leq \omega_c \leq 30$ days to prevent inferring unrealistically small
221 or large values for these parameters for trajectories that were missing data prior to the peak and
222 after the peak, respectively. We also constrained $0 \leq \delta \leq 40$ as Ct values can only take values
223 between 0 and the limit of detection (40).

224
225 We next assumed that the observed $\Delta Ct(t)$ could be described the following mixture model:

$$\Delta Ct(t) \sim \lambda \text{Normal}(E[\Delta Ct(t)], \sigma(t)) + (1 - \lambda) \text{Exponential}(\log(10)) \Big|_0^{\text{l.o.d}}$$

227
228
229 where $E[\Delta Ct(t)] = \text{l.o.d.} - E[Ct(t)]$ and λ is the sensitivity of the q-PCR test, which we fixed at 0.99.
230 The bracket term on the right-hand side of the equation denotes that the distribution was truncated
231 to ensure Ct values between 0 and the limit of detection. This model captures the scenario where

232 most observed Ct values are normally distributed around the expected trajectory with standard
233 deviation $\sigma(t)$, yet there is a small (1%) probability of an exponentially distributed false negative
234 near the limit of detection. The $\log(10)$ rate of the exponential distribution was chosen so that 90%
235 of the mass of the distribution sat below 1 Ct unit and 99% of the distribution sat below 2 Ct units,
236 ensuring that the distribution captures values distributed at or near the limit of detection. We did
237 not estimate values for λ or the exponential rate because they were not of interest in this study;
238 we simply needed to include them to account for some small probability mass that persisted near
239 the limit of detection to allow for the possibility of false negatives.

240
241 We used a hierarchical structure to describe the distributions of ω_p , ω_r , and δ for each individual
242 based on their respective population means μ_{ω_p} , μ_{ω_r} , and μ_{δ} and population standard deviations
243 σ_{ω_p} , σ_{ω_r} , and σ_{δ} such that

244
245 $\omega_p \sim \text{Normal}(\mu_{\omega_p}, \sigma_{\omega_p})$

246 $\omega_r \sim \text{Normal}(\mu_{\omega_r}, \sigma_{\omega_r})$

247 $\delta \sim \text{Normal}(\mu_{\delta}, \sigma_{\delta})$

248
249 We inferred separate population means (μ_{\cdot}) for B.1.1.7- and non-B.1.1.7-infected individuals. We
250 used a Hamiltonian Monte Carlo fitting procedure implemented in Stan (version 2.24)¹⁴ and R
251 (version 3.6.2)¹⁵ to estimate the individual-level parameters ω_p , ω_r , δ , and t_p as well as the
252 population-level parameters σ^* , μ_{ω_p} , μ_{ω_r} , μ_{δ} , σ_{ω_p} , σ_{ω_r} , and σ_{δ} . We used the following priors:

253
254 *Hyperparameters:*

255
256 $\sigma^* \sim \text{Cauchy}(0, 5) [0, \infty]$

257
258 $\mu_{\omega_p} \sim \text{Normal}(14/2, 14/6) [0.25, 14]$

259 $\mu_{\omega_r} \sim \text{Normal}(30/2, 30/6) [2, 30]$

260 $\mu_{\delta} \sim \text{Normal}(40/2, 40/6) [0, 40]$

261
262 $\sigma_{\omega_p} \sim \text{Cauchy}(0, 14/\tan(\pi(0.95-0.5))) [0, \infty]$

263 $\sigma_{\omega_r} \sim \text{Cauchy}(0, 30/\tan(\pi(0.95-0.5))) [0, \infty]$

264 $\sigma_{\delta} \sim \text{Cauchy}(0, 40/\tan(\pi(0.95-0.5))) [0, \infty]$

265
266
267
268
269
270
271
272
273
274
275
276
277
278
279
280
281
282
283
284
285
286
287
288
289
290
291
292
293
294
295

Individual-level parameters:

$$\omega_p \sim \text{Normal}(\mu_{\omega_p}, \sigma_{\omega_p}) [0.25, 14]$$

$$\omega_r \sim \text{Normal}(\mu_{\omega_r}, \sigma_{\omega_r}) [2, 30]$$

$$\delta \sim \text{Normal}(\mu_{\delta}, \sigma_{\delta}) [0, 40]$$

$$t_p \sim \text{Normal}(0, 2)$$

The values in square brackets denote truncation bounds for the distributions. We chose a vague half-Cauchy prior with scale 5 for the observation variance σ^* . The priors for the population mean values (μ) are normally distributed priors spanning the range of allowable values for that parameter; this prior is vague but expresses a mild preference for values near the center of the allowable range. The priors for the population standard deviations (σ) are half Cauchy-distributed with scale chosen so that 90% of the distribution sits below the maximum value for that parameter; this prior is vague but expresses a mild preference for standard deviations close to 0.

We ran four MCMC chains for 1,000 iterations each with a target average proposal acceptance probability of 0.8. The first half of each chain was discarded as the warm-up. The Gelman R-hat statistic was less than 1.1 for all parameters. This indicates good overall mixing of the chains. There were no divergent iterations, indicating good exploration of the parameter space. The posterior distributions for μ_{δ} , μ_{ω_p} , and μ_{ω_r} , were estimated separately for individuals infected with B.1.1.7 and non-B.1.1.7. These are depicted in **Figure 1** (main text). Draws from the individual posterior viral trajectory distributions are depicted in **Supplementary Figure 1**. The mean posterior viral trajectories for each individual are depicted in **Supplementary Figure 2**.

Checking for influential outliers. To examine whether the posterior distributions for the B.1.1.7-infected individuals reflected the influence of a single outlier, we re-fit the model seven times, omitting one of the B.1.1.7 trajectories each time. The inferred parameter values were fairly consistent, though omitting either of two of the B.1.1.7 cases (cases 5 and 6 in **Supplementary Table 2**). yields an infection duration with a 90% credible interval that overlaps with that of the non-B.1.1.7 90% credible interval for infection duration.

296

Standard (copies/ul)	Replicate 1 (Ct)	Replicate 2 (Ct)	Average Ct
10 ⁶	19.3	19.7	19.5
10 ⁵	23.0	21.2	22.1
10 ⁴	26.9	26.7	26.8
10 ³	30.6	30.4	30.5
10 ²	34.0	34.0	34.0
10 ¹	37.2	36.6	36.9
10 ⁰	N/A	39.9	39.9

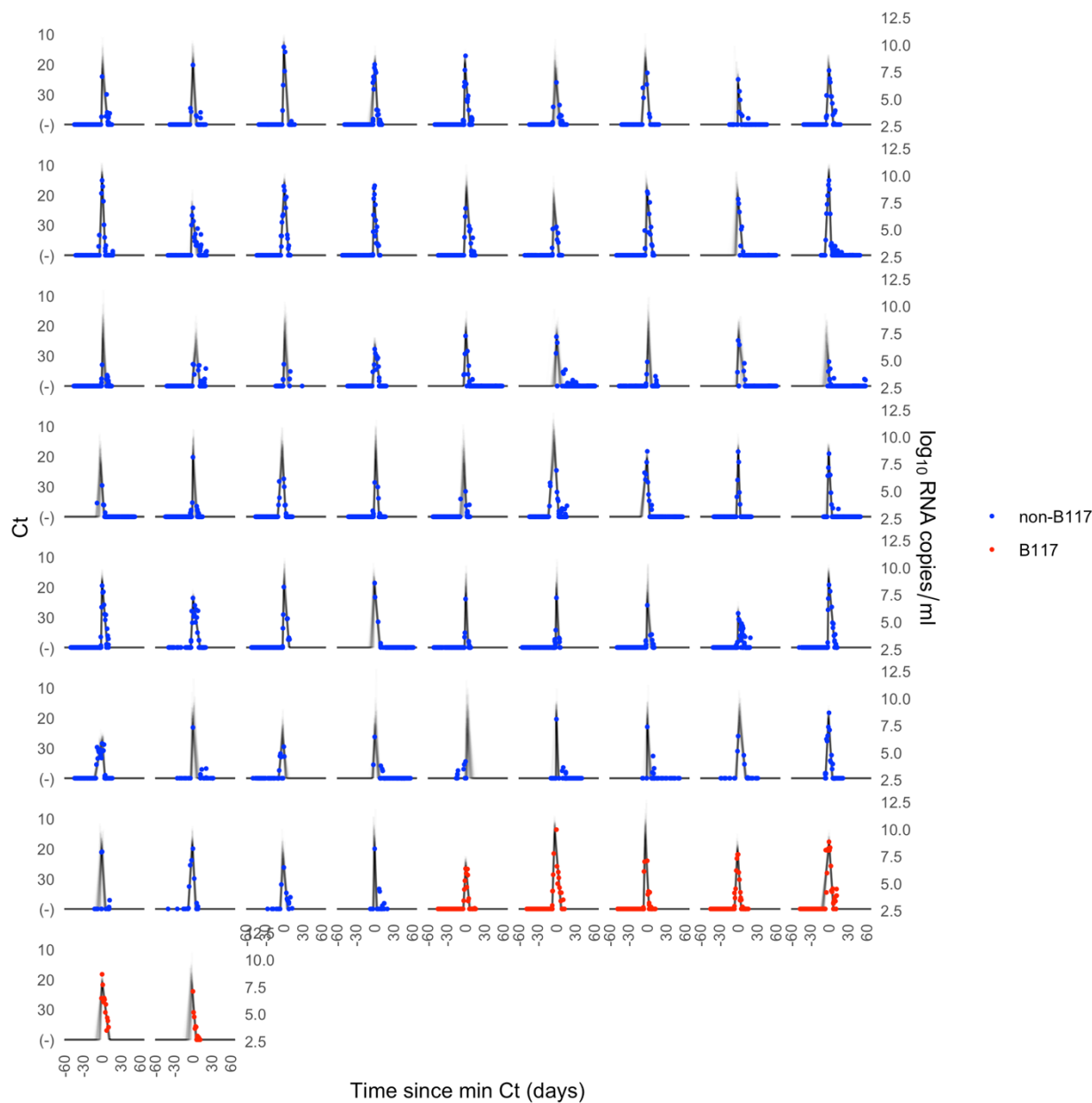
297

298 **Supplementary Table 1. Standard curve relationship between virus RNA copies and Ct values.** Synthetic T7
299 RNA transcripts corresponding to a 1,363 base pair segment of the SARS-CoV-2 nucleocapsid gene were serially
300 diluted from 10⁶-10⁰ and evaluated in duplicate with RT-qPCR. The best-fit linear regression of the average Ct on the
301 log₁₀-transformed standard values had slope -3.60971 and intercept 40.93733 (R² = 0.99).

Omitted B117 Case	Proliferation duration (days) [90% CI]	Clearance duration (days) [90% CI]	Infection duration (days) [90% CI]	Peak viral concentration (log(copies/ml)) [90% CI]
None	5.3 [2.7, 7.8]	8.0 [6.1, 9.9]	13.3 [10.1, 16.5]	8.5 [7.6, 9.4]
1	5.5 [3.0, 8.1]	8.3 [6.3, 10.3]	13.9 [10.6, 17.0]	8.8 [7.9, 9.8]
2	5.7 [3.1, 8.4]	7.5 [5.1, 9.6]	13.2 [9.8, 16.5]	8.2 [7.4, 9.1]
3	5.9 [3.3, 8.6]	8.3 [6.3, 10.3]	14.2 [11.0, 17.4]	8.2 [7.4, 9.1]
4	5.4 [2.7, 7.9]	8.5 [6.3, 10.5]	13.9 [10.5, 17.0]	8.5 [7.6, 9.4]
5	4.3 [1.8, 6.9]	8.3 [6.2, 10.3]	12.6 [9.4, 15.8]	8.4 [7.5, 9.3]
6	5.4 [3.0, 7.9]	7.1 [5.1, 9.1]	12.6 [9.4, 15.6]	8.6 [7.8, 9.6]
7	5.2 [2.6, 7.7]	8.1 [6.0, 10.2]	13.3 [10.1, 16.6]	8.6 [7.8, 9.4]
Non-B.1.1.7 reference	2.0 [0.7, 3.3]	6.2 [5.1, 7.1]	8.2 [6.5, 9.7]	8.2 [7.8, 8.5]

302
303 **Supplementary Table 2. Posterior population mean viral trajectory parameter values and 90% credible intervals**
304 **for B.1.1.7 infections when omitting single trajectories.** Each row corresponds to a model fit obtained by omitting
305 one person who was infected with B.1.1.7, so that the parameter values are informed by six of the seven B.1.1.7
306 infections. The final row lists the fitted parameter values for the non-B.1.1.7 infections for reference.

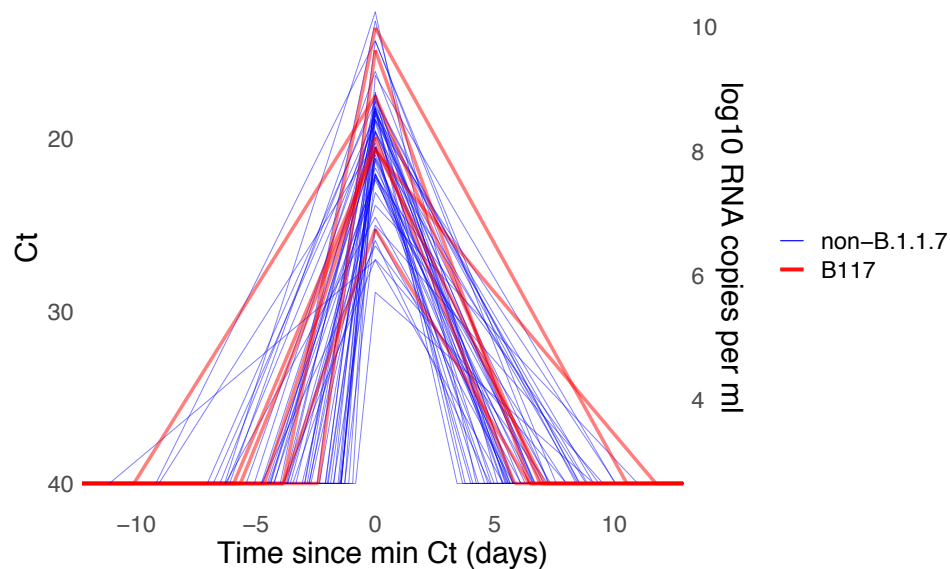
307



308

309

310 **Supplementary Figure 1. Ct values for 65 individuals with estimated viral trajectories.** Each pane depicts the
311 recorded Ct values (points) and derived log-10 genome equivalents per ml ($\log_{10}(\text{ge/ml})$) for a single person during the
312 study period. Points along the horizontal axis represent negative tests. Time is indexed in days since the minimum
313 recorded Ct value (maximum viral concentration). Individuals with confirmed B.1.1.7 infections are depicted in red. Non-
314 B.1.1.7 infections are depicted in blue. Lines depict 100 draws from the posterior distribution for each person's viral
315 trajectory.



316
317
318
319
320
321

Supplementary Figure 2. Mean posterior viral trajectories for each person in the study. Lines depict the posterior mean viral trajectory specified by the posterior mean proliferation time, mean clearance time, and mean peak Ct. Trajectories are aligned temporally to have the same peak time. B.1.1.7 trajectories are depicted in red, non-B.1.1.7 in blue.